



## Adsorption of Basic green 4 from aqueous solution by olive pomace and commercial activated carbon: process design, isotherm, kinetic and thermodynamic studies

Oğuzhan Koçer, Bilal Acemioğlu\*

Science and Art Faculty, Department of Chemistry, Kilis 7 Aralık University, Kilis, Turkey, Tel. +90 348 8222350; Fax: +90 348 8222351; emails: [oguzhankocer@hotmail.com](mailto:oguzhankocer@hotmail.com) (O. Koçer), [acemioglu@kilis.edu.tr](mailto:acemioglu@kilis.edu.tr) (B. Acemioğlu)

Received 31 March 2015; Accepted 2 August 2015

### ABSTRACT

Olive pomace (OP) was used as an adsorbent for the removal of Basic green 4 (BG4) from aqueous solution using adsorption technique. Effects of contact time, adsorbent dose, initial dye concentration, solution pH, and temperature, ionic strength on the adsorption were investigated. Moreover, desorption, isotherm, kinetics, thermodynamics, and process design studies were performed. The adsorption increased with increasing concentration, temperature, and pH, while it was decreasing with the increase in ionic strength. The desorption was highly low in acidic and alkali mediums. Adsorption obeyed the Langmuir, Freundlich, Temkin and Dubinin–Raduskhevich models, and the pseudo-second-order kinetic model. The Langmuir adsorption capacity ( $Q_0$ ) was  $41.66 \text{ mg g}^{-1}$ . The experimental adsorption capacity of the commercial activated carbon was quite high relatively to the OP. A single-stage batch adsorber design was suitable for the usage of the OP in removing of the BG4. Furthermore, Fourier transform infrared, scanning electron microscopy, and thermodynamic studies were also performed.

*Keywords:* Olive pomace; Basic green 4; Activated carbon; Adsorption isotherm; Single-stage batch adsorber design

### 1. Introduction

Adsorption is a physical technique used to remove the undesirable pollutants such as heavy metals, dyes, and pesticides contaminated in wastewaters. Recently, many researchers have preferred to use the low-cost adsorbent materials in the adsorption studies for the removal of undesirable pollutants from wastewaters. Because these materials are highly cheap and economic relatively to the commercial activated carbon. Some of low-cost materials used extensively as adsor-

bent by some researchers can be ranged as: lignin [1], flay ash [2], calabrian pine bark [3–5], pine sawdust [6], peat [7], charcoal ash [8], banana stalk waste [9], wheat brain [10], rice straw-derived char [11], sepiolite [12], dead fungal biomass (*aspergillus wentii*) [13], sea shell powder [14], peanut shell [15,16], raw pine cone biomass (*Pinus radiata*) [17], pineapple leaf powder [18], red mud [19], chitosan [20], papaya seed [21], miswak (*Salvadora Persia*) [22], walnut shell [23], eggshell powder [24], eggshell membrane [25], acetonitrile stannic(IV) selenite composite cation exchanger [26], bottom ash [27], pyrolytic graphite electrode [28], bottom ash and de-oiled soya [29], hen feathers [30,31],

\*Corresponding author.

and modified hibiscus cannabinus fiber [32]. In this study, olive pomace (OP) was selected as an alternative low-cost adsorbent for the removal of Basic green 4 (BG4). On the other hand, commercial activated carbon was also used for the removal of the BG4. Some knowledge's with regard to the OP are given in the following.

Worldwide, 98% of olives is grown in Mediterranean countries, and there are approximately 900 million olives in the areas of more than 10 million hectares [33]. Turkey is one of the Mediterranean countries growing the olive, and the annual amount of the olive oil produced in Turkey is approximately 250,000 tons [34]. On average, 20 kg of the olive oil is extracted from the 100 kg of the olive [33]. The OP is a solid waste which is the remaining portion after the extraction of the olive oil from the olive in the olive oil factories, and it consists of mixture of olive cake and stone [35]. At the same time, the OP is also known under the names of olive cake, olive stone, and pirina. The OP has a heterogeneous property included the olive oil of 6–8%, the water of 20–33%, the seeds, and pulps of 59–74% [33]. The OP is used commonly as a fuel as well as fertilizer and filler in the agriculture [35]. Recently, the OP has also been used as an adsorbent for the removal of heavy metal and dye pollutants from wastewaters. However, the adsorption studies of heavy metals and dyes onto the OP are restricted in literature. Some of the metal and dye adsorption works done with the OP are summarized in the following.

For example, Pagnanelli et al. have used OP as an adsorbent for the removal of copper, lead, and cadmium [36]. Kula et al. have studied the removal of cadmium from aqueous solution using the olive stones impregnated with  $ZnCl_2$  and carbonized at 650 °C under nitrogen atmosphere [37]. Aziz et al. have investigated the removal of cadmium and safranin using the olive stone treated with sulfuric acid [38]. Rouibah et al. have studied the removal of Chromium (VI) and Cadmium(II) from aqueous solutions by the olive stones [39]. On the other hand, the adsorption kinetics and thermodynamics of iron III ions onto the olive stones have been studied by Martinez-Nieto et al. [40] and Hodaifa et al. [41].

Moreover, a few works of dye adsorption done with the OP have also been performed. For instance, the OP activated with  $ZnCl_2$  have been used as an adsorbent for the adsorption of an anionic dye Remazol red B from aqueous solution by Uğurlu et al. [42]. Akar et al. have studied the adsorption of Reactive Red 198 by untreated OP [43]. Baccar et al. have also studied the adsorption of Lanaset Grey, an industrial metal complex dye, by activated carbon produced

from the olive-waste cake [44]. On the other hand, in our a work, we have investigated the adsorption of methyl violet by the pirina [45]. In another work, we have studied the removal of remazol brilliant blue R from aqueous solution using the pirina and commercial activated carbon [46].

Any work on the adsorption of Basic Green 4 (BG4), a cationic dye, on the OP has not been met in the literature, so far. The BG4 is a toxic dye, having genotoxic, mutagenic, teratogenic, and carcinogenic effects. If the BG4 is discharged to environment, it threatens the health of animals and humans. For example, when this dye comes into contact with human, it causes damage to the liver, spleen, and kidney. On the other hand, it leads lesions on skin, eyes, lungs, and bones [18]. Therefore, in this study, we have aimed the removal of the BG4 from aqueous solution using the OP as an adsorbent. The effects of contact time, adsorbent dose, initial dye concentration, solution pH, and temperature, ionic strength on the adsorption of the BG4 were investigated, respectively. Moreover, desorption, isotherm, kinetics, thermodynamics, process design, XRD, scanning electron microscopy (SEM), and Fourier transform infrared (FT-IR) studies were performed. On the other hand, the commercial activated carbon (CAC) was also used for the adsorption of the BG4. The obtained findings were discussed in detail.

## 2. Materials and methods

### 2.1. Materials

#### 2.1.1. Adsorbent

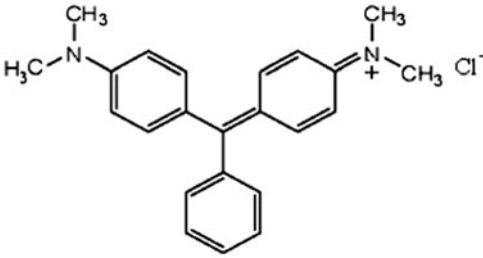
The OP wastes used for the experiments was received from a private olive oil factory in Kilis city located in the southern part of Turkey. The CAC (Code Number: 434454) was provided from the Carlo Erba firm. Both adsorbents were utilized without any pre-treatment in the adsorption experiments.

#### 2.1.2. Adsorbate

The BG4, a cationic dye (C. I. 42000) was provided from Merck. It was used as received without further purification in the experiments. The chemical structure and some physical properties of the BG4 are given in Table 1. In order to obtain the desired concentrations, the stock solutions of 500-mg dye  $L^{-1}$  were prepared with distilled pure water. Initial pH values of the dye solutions prepared were adjusted using 0.1 N HCl and NaOH solutions.

Table 1

Chemical structure and some physical properties of the BG4

Common name	Malachite green
Other name	Aniline green; Basic green 4; Diamond green B; Victoria green B
IUPAC name	4-[(4-dimetilaminofenil)fenil-metil]-N,N dimetilanolin
Chemical formula	$C_{23}H_{25}ClN_2$
Class	Basic
Color index	42,000
Molecular weight ( $g\ mol^{-1}$ )	36,491
Solubility in water ( $g\ L^{-1}$ )	25°C'de 40
Solubility in ethanol	Good
Colors at different pH (indicator property)	Green-blue in water Yellow < pH 2 Green at pH 2 Colorless at pH 14
$\lambda_{max}$ (nm)	617
Molecular structure	

## 2.2. Methods

### 2.2.1. Adsorption studies

Firstly, the samples of the OP were dried in an oven at 100°C for 6 h to remove the moisture before experiments, and then they were passed over a 100-mesh molecular sieve for the adsorption experiments. The adsorption experiments were conducted by stirring 0.50 g of the OP with the BG4 solution of 100 mL in 250-mL erlenmeyer flasks placed on a temperature-controlled magnetic stirrer for various concentrations (between 20 and 100  $mg\ L^{-1}$ ), pHs (between 3 and 8), temperatures (between 20 and 50°C), adsorbent doses (between 0.25 and 2.0 g), and ionic strengths (between 0.05 and 0.3 M) as a function of contact time at a constant shaking rate of 400 rpm. After the desired contact times, the samples were withdrawn from mixture using a micropipette to prevent the transition of the OP particles to the solution, and then they were centrifuged for 5 min at 3,000 rpm. After centrifuged, the supernatants were analyzed for the determination of the final concentration of the BG4 by using an T80 UV-vis spectrophotometer set at a wavelength of 617 nm, maximum absorbance. The amounts of dye adsorbed by the OP were calculated from difference between final and initial concentrations. All the

experiments were carried out in twice, and the average results were evaluated.

### 2.2.2. Desorption studies

The samples of the dye-loaded OP was gently washed with water to remove any unadsorbed dye. Then these were stirred on a magnetic stirrer with 100 mL of 0.1 N HCl solution, of the distilled waters at different pHs and of an acetone-water mixture of 50% for 30 min, one by one [46]. The amounts of the BG4 passing from the surface of the OP into the liquid phase were calculated using a UV-vis spectrometer as before.

### 2.2.3. Characterization of adsorbent

For the characterization of adsorbent, firstly, the OP samples were dried to the constant weight in an oven at 60°C for 12 h. The elemental analysis of the OP was performed using a LECO CHNS-932 analyzer, and also its the chemical composition was determined according to methods mentioned elsewhere [47,48]. A FT-IR spectra were recorded in the wave number range of 4,000–650  $cm^{-1}$  using an ATR spectrophotometer (FTIR RX-1, Perkin Elmer). A SEM analysis was performed using a (LEO 435 VP SEM). The XRD

spectra was done by an X-ray diffractometer (Rigaku RadB-DMAX II) using Cu K $\alpha$  radiation at 40 kV and 40 mA at 2 $\theta$  between 0 and 80°.

### 3. Results and discussion

#### 3.1. Characterization of the adsorbent

##### 3.1.1. Elemental analysis and chemical composition of the OP

The chemical composition of the OP consists of 37.06% cellulose, 29.39% hemicellulose, 33.65% lignin, 66.45% holocellulose, 3.58% ash, and 21.30% extractive matter (alcohol-benzen). According to elemental analysis results, it includes 53.23% C, 37.39% O, 7.13% H, and 2.25% N.

##### 3.1.2. Surface area and XRD analysis of the OP

The BET and Langmuir surface areas of the OP were determined as 0.018 and 0.0704 m<sup>2</sup> g<sup>-1</sup>, respectively. On the other hand, and total volume and area in pores of the OP were found to be 0.00004 cm<sup>3</sup> g<sup>-1</sup> and 0.042 m<sup>2</sup> g<sup>-1</sup>, respectively. XRD analysis of the OP was done before and after adsorption. XRD spectra obtained are given in Fig. 1.

From Fig. 1(a), it is seen that any XRD peak for the OP could not be obtained. After the adsorption, the diffraction peak did not almost change (Fig. 1(b)). This indicates to the amorphous and irregular nature of the OP. A similar result has been recorded for the adsorption of Lanaset Grey G (a metal complex dye) onto activated carbon prepared from Tunisian olive-waste cake [44].

##### 3.1.3. FT-IR analysis

In order to better understand the nature of the functional groups on the surface of the OP responsible for the adsorption of the BG4, the FT-IR spectra of the OP were recorded. Before and after the adsorption, the FT-IR spectra of the OP obtained are shown in Fig. 2.

As seen in Fig. 2, the broad and strong peak between 3,400 and 3,200 cm<sup>-1</sup> indicates the existences of OH groups of cellulose and the stretching vibration of N-H and NH<sub>2</sub> groups [15,48]. This band at 3,330.20 cm<sup>-1</sup> is not changed after the adsorption of the BG4. The strong absorption bands between 2,921.53 and 2,852.19 cm<sup>-1</sup> can be assigned to symmetric and asymmetric stretching of methyl and methylene groups [9]. These peaks did not almost change after the adsorption of the BG4. The bands between

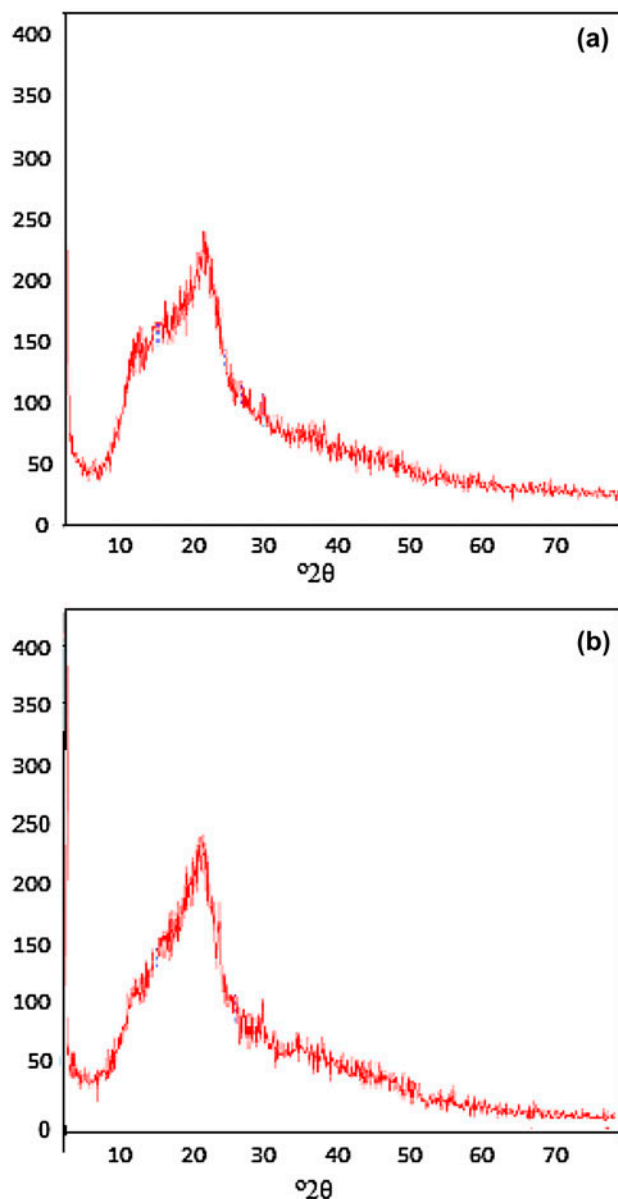


Fig. 1. XRD spectra of the OP: (a) before adsorption and (b) after adsorption.

1,710.19 and 1,626.46 cm<sup>-1</sup> indicate to amide I and amide II bands of protein peptide bonds [16]. After the adsorption, the intensity of this band at 1,710.19 cm<sup>-1</sup> increased, and also the band at 1,626.46 cm<sup>-1</sup> shifted to 1,613.42 cm<sup>-1</sup>. On the other hand, the peak at 1,232.32 cm<sup>-1</sup> points to the C=O stretching of carboxylic groups [16,49]. After the adsorption, this peak shifted very slightly to 1,236.08 cm<sup>-1</sup>. The peaks at around 1,200–1,000 cm<sup>-1</sup> indicate to the existence of C–O single bond in carboxylic acids, alcohols, phenols, and esters [15,39]. Herein, a very strong absorption peak at 1,030.19 cm<sup>-1</sup>

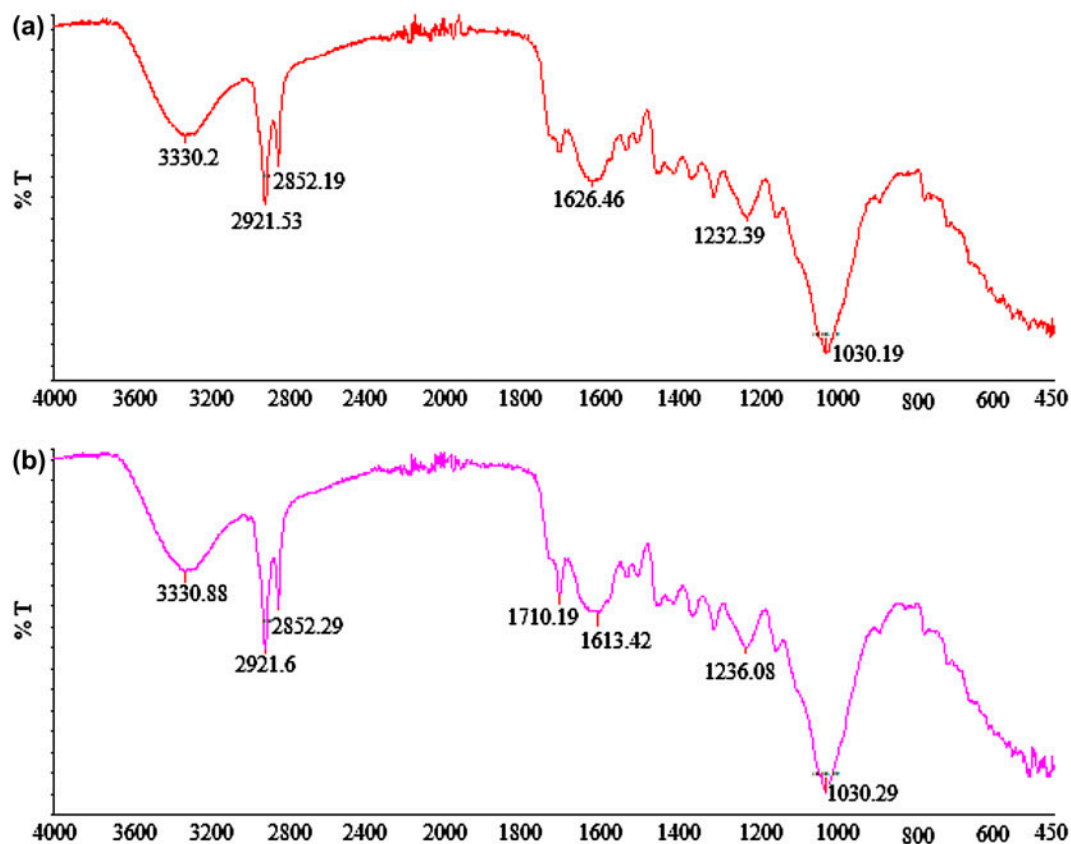


Fig. 2. FT-IR spectra of the OP: (a) before adsorption and (b) after adsorption.

can be assigned to C–O bonds in phenolic and carboxylic groups. This band did not change after the adsorption, also. All these findings show that the OP has characteristic bonds of proteins, phenolic, and carboxylic groups, polymeric compounds which are able to adsorb BG4 molecules in aqueous solution.

#### 3.1.4. SEM analysis

Before and after adsorption, the SEM images of the dried samples of both the OP and the dye-loaded OP are illustrated in Fig. 3.

The image in Fig. 3(a) shows that the surface has some pores and caves within the particles of the OP. If it is noticed to Fig. 3(b), it is seen that the surface of the OP is remarkably coated with the molecules of BG4, and this situation indicates a surface adsorption.

#### 3.2. Determination of adsorption equilibrium time

Determination of the adsorption equilibrium time in an adsorption process is a very important issue. Herein, the equilibrium time was determined as a function of contact time. Therefore, the effect of contact

time on the adsorption of the BG4 on the OP was investigated under all the experimental conditions such as initial dye concentration, solution pH, and temperature for various contact times (1, 3, 5, 10, 15, 30, 60, 90, and 120 min). From the results obtained, it was seen that a rapid adsorption of the BG4 occurred in a short time of 3–5 min and then a gradual increase in the adsorption maintained up to 120 min. After this time, the amount of the adsorption did not change with an increase in contact time. Therefore, this time was accepted as an equilibrium time. In the next experiments, the isotherm, kinetic, and thermodynamic studies of the adsorption process were performed by using the equilibrium data. On the other hand, the similar results for rapid adsorption within a very short contact of times have also been recorded for the adsorption of Malachite green onto neem sawdust [50] and beech sawdust [51].

#### 3.3. Effect of adsorbent dose on the adsorption of the dye

The effect of adsorbent dose on the adsorption of the BG4 on the OP was studied at five different doses of 0.25, 0.5, 1.0, 1.5, and 2.0 g for the initial dye

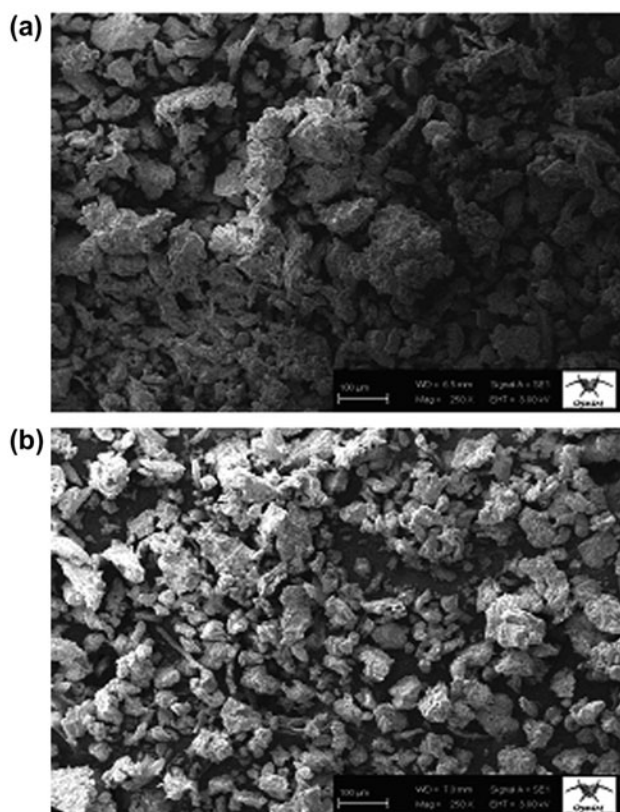


Fig. 3. SEM image of the OP: (a) before adsorption and (b) after adsorption.

concentration of  $100 \text{ mg L}^{-1}$  at pH 4.5,  $25^\circ\text{C}$  and 400 rpm, respectively. The results obtained are shown in Fig. 4.

From Fig. 4(a), it was seen that a rapid adsorption occurred in a first few min and then a gradual increase in the adsorption maintained up to 120 min as a function of contact time for each adsorbent dose. The amounts of the BG4 adsorbed per unit mass of the OP were found to be higher at lower dose and lower at higher dose. At the same time, the amount of an adsorbate adsorbed per unit mass of an adsorbent can also be expressed as unit adsorption (UA). The UA is equal to the ratio of the amount of adsorbate adsorbed/the adsorbent dose. Therefore, the UA is higher at lower adsorbent dose. Fig. 4(b) shows the relationship between the UA and the percent adsorption (PA) for various adsorbent doses at equilibrium time. It can be seen from Fig. 4(b) that there is an opposite effect between the UA and the PA. If it is noticed to this figure, it can be seen that the PA increases while the UA decreases at higher adsorbent dose. Because, the higher adsorbent dose has more active site on the surface of the adsorbent, causing the higher percentage of the dye adsorption. A similar

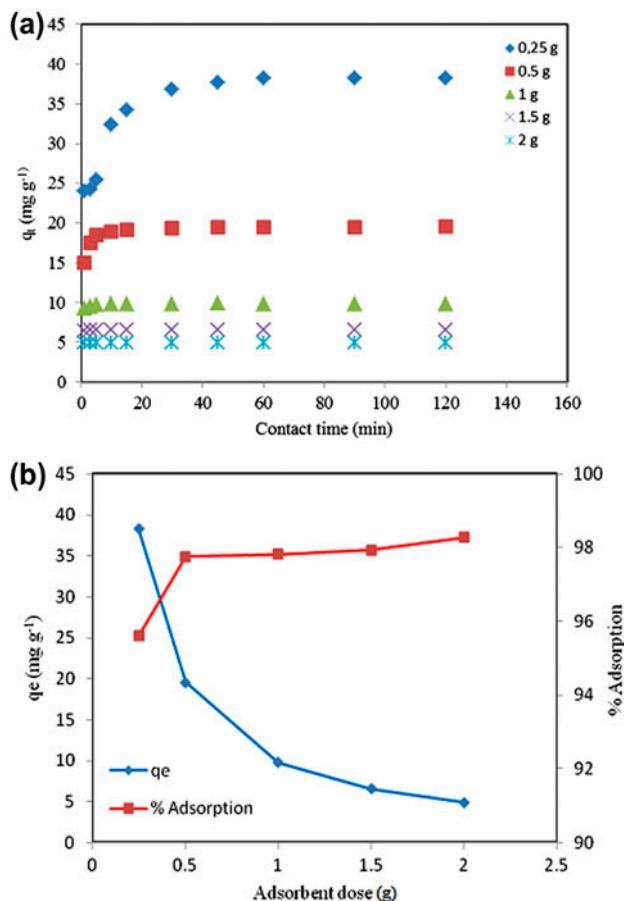


Fig. 4. Effect of adsorbent dose on the adsorption: (a) effect of adsorbent dose on the adsorption and (b) relationship between the UA and the PA for various adsorbent doses at equilibrium time.

result has also been recorded for the adsorption of the BG4 onto sea shell powder [14].

### 3.4. Effect of the initial concentration on the adsorption of the dye

The initial concentrations for the adsorption of the BG4 on the OP were selected as 20, 40, 60, 80, and  $100 \text{ mg L}^{-1}$  at pH 4.5,  $25^\circ\text{C}$  and 400 rpm, respectively. The effect of the initial concentration on the adsorption of BG4 on the OP is shown in Fig. 5.

As seen from Fig. 5 that a rapid adsorption occurred within a few minutes, and then a gradual increase in the adsorption maintained up to 120 min for all concentrations. For the initial concentrations of 20, 40, 60, 80, and  $100 \text{ mg L}^{-1}$ , while the adsorption of the BG4 on the OP were  $3.54 \text{ mg g}^{-1}$  (88.43%),  $6.26 \text{ mg g}^{-1}$  (78.24%),  $9.96 \text{ mg g}^{-1}$  (83%),  $13.94 \text{ mg g}^{-1}$  (87.10%), and  $14.97 \text{ mg g}^{-1}$  (74.87%) at 1 min, the

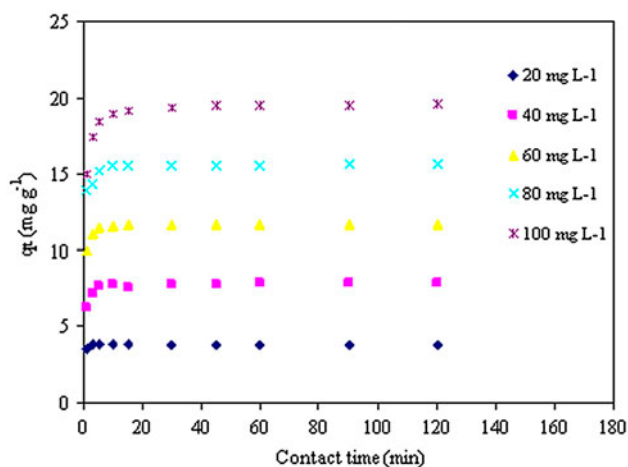


Fig. 5. Effect of initial concentration on the adsorption.

maximum adsorption were found as  $3.88 \text{ mg g}^{-1}$  (96.90%),  $7.84 \text{ mg g}^{-1}$  (98.0%),  $11.23 \text{ mg g}^{-1}$  (97.74%),  $15.58 \text{ mg g}^{-1}$  (97.43%), and  $19.55 \text{ mg g}^{-1}$  (97.75%) at 120 min, respectively. From these values, it was seen that the PA increased, while the maximum amount of the BG4 adsorbed was increasing with an increase in the initial concentration of the dye. This situation may probably indicate to a shift in the adsorption equilibrium. A similar result has also been recorded for the adsorption of Congo red on calcium-rich fly ash [2].

### 3.5. Effect of solution pH on the adsorption of the dye

The pH values of the initial solution for the adsorption of the BG4 on the OP were adjusted as 3, 4.5, 7, and 8 for the initial concentration of  $100 \text{ mg L}^{-1}$  at  $25^\circ\text{C}$  and 400 rpm, respectively. The effect of the initial solution pH on the adsorption of the BG4 on the OP is illustrated in Fig. 6.

From Fig. 6, as to be in the concentration effect, it was seen that a rapid adsorption occurred within first a few minutes for all pH values. Moreover, it was seen that the highest adsorption occurred at pH 8, while the lowest adsorption taking place at pH 3. For instance, while the adsorption of the BG4 on the OP were  $11.76 \text{ mg g}^{-1}$  (58.79%),  $14.97 \text{ mg g}^{-1}$  (74.87%),  $15.53 \text{ mg g}^{-1}$  (77.65%), and  $15.74 \text{ mg g}^{-1}$  (78.72%) at 1 min, the maximum adsorption were determined as  $17.78 \text{ mg g}^{-1}$  (88.92%),  $19.55 \text{ mg g}^{-1}$  (97.75%),  $19.54 \text{ mg g}^{-1}$  (97.69%) and  $19.48 \text{ mg g}^{-1}$  (97.41%) at pH values of 3, 4.5, 7, and 8 at 120 min, respectively. Herein, we can clarify the effect of pH on the adsorption. The pH value of the solution affects both the chemical structure of an adsorbent and the ionization of a dye molecule. Because, the excess  $\text{OH}^-$  ions is

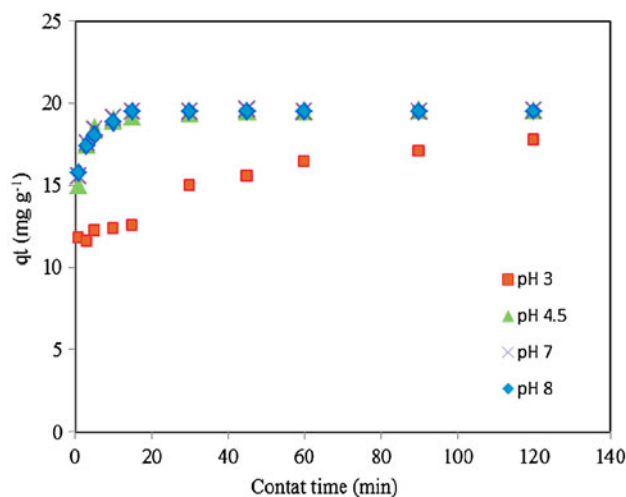


Fig. 6. Effect of pH on the adsorption.

released into the solution in a higher pH medium while the excess  $\text{H}^+$  ions is released into the solution in a lower pH medium. The chemical structure of the OP consists of the various groups such as cellulose, hemicellulose, lignin, amine, phosphate, and some extractive materials. These groups have become more negatively charged in the higher pH medium, and they lead to a higher adsorption via the electrostatic interactions with positively charged BG4 molecules. A similar result has also been recorded for the adsorption Malachite green onto rattan sawdust [52]. On the other hand, the determination of surface charge of the adsorbent is also important to obtain better information about the adsorption. Therefore, the surface charge of the OP was estimated by measuring the zeta potential of its suspension at different pH values of the medium (between pH 2 and 10). The potential of zeta was found to be between 4.12 and  $-12.85 \text{ mV}$  for medium pHs between pH 2 and 10. However, zeta potential has negative values over about pH 2.3. This situation indicates to negative charge density on the surface of the OP, probably deprotonating of phenolic and carboxylic groups. This charge density was observed to increase with the increasing medium pH. In this study, the lower adsorption was obtained at pH 3, and after this pH the adsorption was observed to be increased due to the increase in the negative charge density of the surface of the OP.

### 3.6. Effect of solution temperature on the adsorption of the dye

The solution temperatures for the adsorption of the BG4 on the OP were selected as 20, 30, 40, and  $50^\circ\text{C}$

for the initial concentration of  $100 \text{ mg L}^{-1}$  at pH 4.5 and 400 rpm, respectively. The effect of temperature on the adsorption of the BG4 on the OP is shown in Fig. 7.

From Fig. 7, as to be in the concentration and pH effects, it was seen that a rapid adsorption took places within first a few minutes for all temperatures. Then, a gradual increase in the adsorption maintained up to 120 min for all temperature. For example, for the various temperatures of 20, 30, 40, and  $50^\circ\text{C}$ , while the adsorption of the BG4 on the OP were  $14.97 \text{ mg g}^{-1}$  (74.87%) and  $17.75 \text{ mg g}^{-1}$  (88.77%),  $18.11 \text{ mg g}^{-1}$  (90.54%), and  $18.83 \text{ mg g}^{-1}$  (94.18%) at 1 min, the maximum adsorption were found to be  $19.55 \text{ mg g}^{-1}$  (97.75%),  $19.58 \text{ mg g}^{-1}$  (97.90%),  $19.59 \text{ mg g}^{-1}$  (97.96%), and  $19.61 \text{ mg g}^{-1}$  (98.10%) at 120 min, respectively. From these values, it was observed that a slight increased in adsorption occurs with increasing temperature. Namely, an increase in temperature was in favor of dye adsorption and indicated to an endothermic process. A similar result has also been recorded for the adsorption of Malachite green onto beech sawdust [51].

### 3.7. Effect of ionic strength on the adsorption of the dye

The effect of ionic strength on the adsorption of BG4 on the OP was studied in the presence of NaCl, KCl, and  $\text{CaCl}_2$  salts with the ionic strength concentrations of 0.05, 0.10, 0.20, and 0.30 M ( $\text{mol L}^{-1}$ ). The results obtained are shown in Fig. 8.

From this figure, it was seen that the adsorption of the BG4 decreased in the presence of NaCl, KCl, and  $\text{CaCl}_2$ . With the addition of NaCl, KCl, and  $\text{CaCl}_2$  into the solution, the salts dissociate into their ions (namely

$\text{Na}^+$ ,  $\text{K}^+$ ,  $\text{Ca}^{2+}$ ,  $\text{Cl}^-$  ions). These ions hindered the adsorption of positively charged BG4 molecules onto the OP, and they led to an decrease in the adsorption. While this decrease was lower in the presence of NaCl and KCl, it was higher in the presence of  $\text{CaCl}_2$  possessing higher ionic strength (see Fig. 8). This situation may be explained in two ways: firstly since ionic strength of calcium is four times more than that of sodium and potassium, calcium ions may more hinder the orientation of BG4 molecules to surface of the OP. Secondly, in the presence of calcium, the surface of the OP may become more positively charged, and consequently more repulsion may occur between the surface of the OP and positively charged BG4 molecules according to the presence of sodium and potassium. In no case of salt in medium, the PA was found to be 97.75%. Similar results have also been recorded for the adsorption of Rhadamine B and Methylene Blue onto *Fomes fomentarius* and *Phellinus igniarius* which are bioadsorbents prepared from dead macro fungi [53].

### 3.8. Adsorption of the BG4 onto the CAC

The CAC was also utilized for the adsorption of the BG4. The ratios of the CAC to liquid dye solution (LDS) were selected as 0.05 g/100 mL, 0.10 g/100 mL, 0.25 g/100 mL, 0.50 g/100 mL, 1.0 g/100 mL, and 1.50 g/100 mL, respectively. The adsorption capacity obtained of CAC for the adsorption of the BG4 was compared with the adsorption capacity of the OP. For all concentrations, PA was found as 100%. At the same time, it was seen that the color of the BG4 turned to colorless within a very short time of 1–2 min. These results indicate that the CAC has a

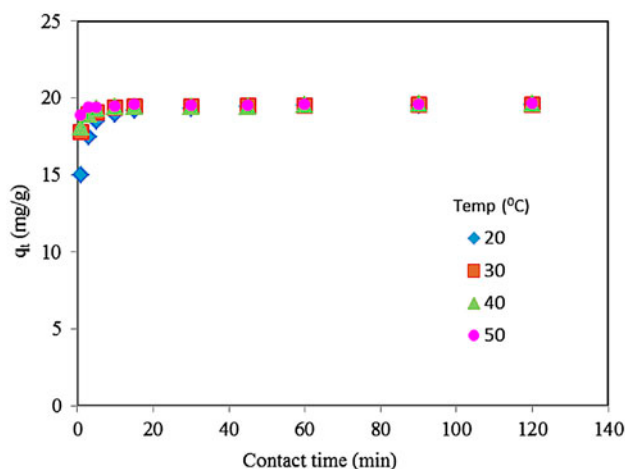


Fig. 7. Effect of temperature on the adsorption.

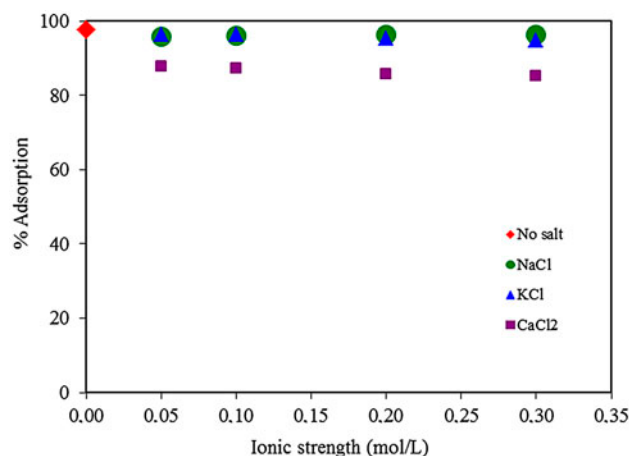


Fig. 8. Effect of ionic strength on the adsorption.



very high adsorbing effect than the OP for the adsorption of the BG4.

### 3.9. Isotherm Studies

The adsorption isotherm were studied using the equilibrium data obtained for the initial dye concentrations of 40, 50, 60, 70, and 80 mg L<sup>-1</sup> at pH 4.5, 25°C and 400 rpm. The adsorption isotherm of the BG4 onto the OP was studied according to the Langmuir, the Freundlich, the Temkin, and the Dubinin–Radushkevich (D–R) models, respectively. The linearized equations of these isotherms can be expressed as follows, respectively [2,54–56].

$$C_e/q_e = 1/Q_o b + C_e/Q_o \quad \text{Langmuir} \quad (1)$$

$$\ln q_e = \ln k + 1/n \ln C_e \quad \text{Freundlich} \quad (2)$$

$$q_e = B \ln A_T + B \ln C_e \quad \text{Temkin} \quad (3)$$

$$\ln q_e = \ln X'_m - K' \varepsilon^2 \quad \text{Dubinin–Radushkevich} \quad (4)$$

where  $q_e$  is the amount of the dye adsorbed at the equilibrium time (mg g<sup>-1</sup>),  $C_e$  is the concentration of the dye remained in solution at the equilibrium time (mg L<sup>-1</sup>).  $Q_o$  and  $b$  show the Langmuir constants which indicate to the adsorption capacity and energy, respectively.  $k$  and  $n$  are the Freundlich constants denoting the capacity and intensity of the adsorption, respectively.  $B$  is a constant indicating the heat of the adsorption (J mol<sup>-1</sup>), and it is equal to  $RT/b_T$ .  $b_T$  is Temkin constant, and  $A_T$  is equilibrium binding constant (L g<sup>-1</sup>).  $T$  is absolute temperature (K),  $R$  is an ideal gas constant (J mol<sup>-1</sup> K<sup>-1</sup>).  $\varepsilon$  is Polanyi potential and it is equal to  $RT \ln(1 + 1/C_e)$ .  $X'_m$  indicates to the adsorption capacity (mg g<sup>-1</sup>).  $K'$  is a constant showing the adsorption energy (mol<sup>2</sup> J<sup>-2</sup>).  $E$  indicates to the mean adsorption energy per molecule of the adsorbate, and it is given as  $E = 1/(2K')^{1/2}$ . All of the isotherm graphs obtained are shown in Fig. 9.

All of the isotherm parameters obtained from regression analyses of all plots shown in Fig. 9 are given in Table 2.

The values of  $Q_o$  and  $b$  were calculated from the slope and the intercept of the plot of  $C_e/q_e$  against  $C_e$  using the Langmuir equation, respectively. The values of  $Q_o$  and  $b$  were calculated as  $40.90 \pm 1.83$  mg g<sup>-1</sup> and  $0.30 \pm 0.02$  L mg<sup>-1</sup>, respectively. Its correlation coefficient ( $R^2$ ) was found as 0.997. On the other hand, the Langmuir adsorption capacity ( $Q_o$ ) obtained was compared to some other adsorbents, and they are given in Table 3.

The values of  $k$  and  $n$  were determined from the slope and the intercept of the plot of  $\ln k$  vs.  $\ln C_e$  using the Freundlich equation. The values of  $k$  and  $n$  were determined to be  $9.40 \pm 0.04$  mg g<sup>-1</sup> and  $1.38 \pm 0.08$  g L<sup>-1</sup>, respectively. The  $R^2$  was found as 0.994. The values of  $B$  and  $A_T$  were estimated from the slope and the intercept of the plot of  $q_e$  vs.  $\ln C_e$  using the Temkin equation. The values of  $B$  and  $A_T$  were found to be  $8.14 \pm 0.21$  (J mol<sup>-1</sup>) and  $3.24 \pm 0.08$  (L g<sup>-1</sup>), respectively and the  $R^2$  was determined as 0.994. The values of  $K'$  and  $X'_m$  were calculated from the slope and the intercept of the plot of  $\ln q_e$  vs.  $\varepsilon^2$  using the D–R equation, respectively. The values of  $K'$  and  $X'_m$  were calculated to be  $2.10^{-7} \pm 0.0$  mol<sup>2</sup> J<sup>-2</sup> and  $18.47 \pm 0.43$  mg g<sup>-1</sup>, respectively. The  $R^2$  was determined as 0.987.

As seen in Table 3, the fact that the values of the  $R^2$  obtained from all isotherm equations were 0.991 and 0.996 indicated that the adsorption was in consistent with these models. A similar result has also been recorded for the adsorption of Malachite green onto bentonite [57]. The fact that the adsorption obeys the Langmuir isotherm indicates to be the uniform of binding energy and the homogeneous adsorption on the surface of the OP. A similar result has also been reported for the adsorption of the BG4 on the surface of sea shell powder [14]. The fact that the adsorption obeys the Freundlich and the D–R isotherms indicates to the heterogeneous adsorption on the surface of the OP. On the other hand, the D–R isotherm gives information about a physical or chemical adsorption, also [55]. Herein, from the D–R isotherm the value of the mean adsorption energy ( $E$ ) per molecule of the OP was found to be 1.58 kJ mol<sup>-1</sup>, indicating a physical adsorption. A similar result has also been recorded for the adsorption of the BG4 on the surface of sea shell powder [14]. The fact that the adsorption obeys the Temkin isotherm indicates to the decrease in the adsorption heat with the increasing dye coverage of the surface of the OP [56].

### 3.10. Desorption of BG4 from the surface of the OP

Desorption studies was done to determine the desorption degree of the BG4 from the surface of the OP. The desorption experiments were performed using various alkali waters at pH values of 5.0, 7.0, 9.0, and 10, an acetone-water mixture of 50%, and 0.10 N HCl solution (pH 1.27), respectively. For this purpose, the dye-loaded OP was stirred with 100 mL of all solutions for 30 min, one by one. The desorption graph is shown in Fig. 10.

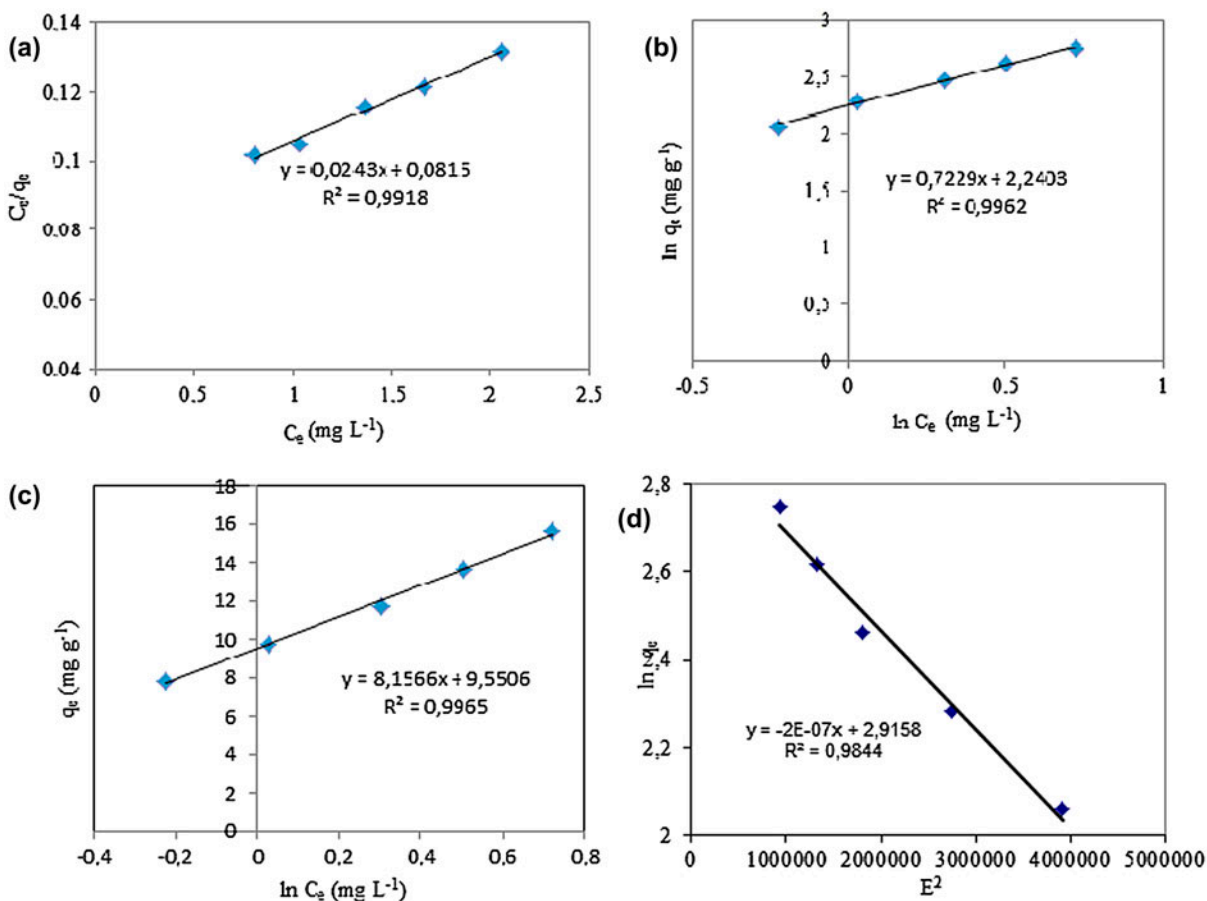


Fig. 9. The isotherm plots of the adsorption: (a) the Langmuir isotherm, (b) the Freundlich isotherm, (c) the Temkin isotherm, and (d) the D–R isotherm.

Table 2

Isotherm parameters for the adsorption of the BG4 onto the OP

Langmuir	Freundlich	Temkin	Dubinin–Radushkevich
$Q_o$ ( $\text{mg g}^{-1}$ ) = $40.90 \pm 1.83$	$k$ ( $\text{mg g}^{-1}$ ) = $9.40 \pm 0.04$	$B$ ( $\text{J mol}^{-1}$ ) = $8.14 \pm 0.21$	$X'_m$ ( $\text{mg g}^{-1}$ ) = $18.47 \pm 0.43$
$b$ ( $\text{L mg}^{-1}$ ) = $0.30 \pm 0.016$	$n$ ( $\text{g L}^{-1}$ ) = $1.38 \pm 0.025$	$A_T$ ( $\text{L g}^{-1}$ ) = $3.24 \pm 0.08$	$K'$ ( $\text{mol}^2 \text{J}^{-2}$ ) = $2 \times 10^{-7} \pm 0.0$
$r^2 = 0.997$	$r^2 = 0.994$	$r^2 = 0.994$	$r^2 = 0.987$

It can be seen from this figure that the percent desorption (PD) was very low in 0.10 N HCl solution and in alkali water mediums. For example, the PD was found as 3.29% in 0.10 N HCl solution, indicating not to be any ion-exchange mechanism between the OP and the BG4. On the other hand, the PD was found between 0.52 and 0.81 in alkali waters between pH 5 and 10. The low desorption indicated that a chemical adsorption might be occurred between the OP and the BG4 molecules. In the case of an acetone water mixture of 50%, a desorption of 42.40% was observed.

### 3.11. Kinetic studies

The adsorption kinetics were studied for the initial dye concentrations of 20, 40, 60, 80, and 100  $\text{mg L}^{-1}$  at pH 4.5 and 25 °C and 400 rpm, respectively. The kinetics of the adsorption of the BG4 onto the OP were studied in terms of the pseudo-first-order kinetic model [58], the pseudo-second-order kinetic model [59,60], the intraparticle diffusion model [61] and the Elovic kinetics [57,62]. The linearized equations of these kinetic models can be expressed as follows, respectively.

Table 3  
Comparison of the Langmuir adsorption capacity ( $Q_o$ ) to some other adsorbents

Adsorbent/biosorbent	Adsorbate dye	$Q_o$ (mg g <sup>-1</sup> )	Refs.
Olive pomace	Basic green 4	41.66	This study
Sea shell powder	Basic green 4	42.33	[14]
Pineapple	Basic green 4	54.64	[18]
Walnut shell	Malachite green	90.80	[23]
Neem sawdust	Malachite green	4.35	[50]
Rattan sawdust	Malachite green	62.71	[52]
Dead leaves of plane tree	Malachite green	85.47	[62]
Acid-activated low-cost carbon	Malachite green	9.73	[64]
Zeolite	Malachite green	23.94	[67]
Rice husk-activated carbon	Malachite green	63.85	[68]
Bentonite	Malachite green	7.72	[69]

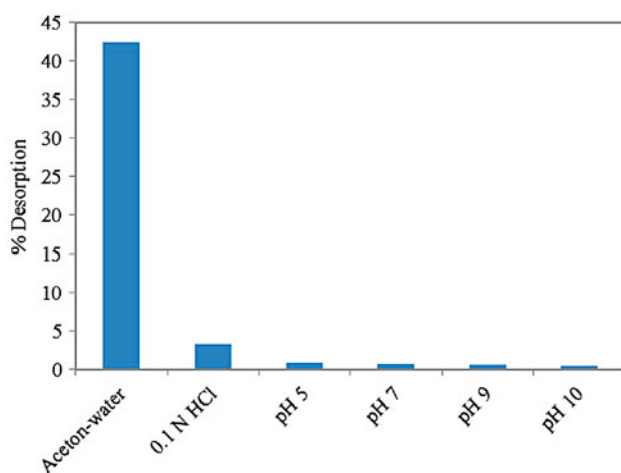


Fig. 10. Desorption of the BG4 from the OP.

$$\log(q_e - q_t) = \log q_e - \frac{k_1}{2.303} t \quad (5)$$

$$\frac{t}{q_t} = \frac{1}{h} + \frac{1}{q_e} t \quad (6)$$

$$q_t = k_1 t^{1/2} \quad (7)$$

$$q_t = 1/\beta \ln(\alpha\beta) + 1/\beta \ln t \quad (8)$$

where  $t$  is contact time (min),  $q_e$  and  $q_t$  are the amounts of dye adsorbed per unit mass of adsorbent at the equilibrium and any time (mg g<sup>-1</sup>), respectively. The  $h$  in Eq. (6) indicates to the initial adsorption rate (mg g<sup>-1</sup> min), and it is expressed as  $h = k_2 q_e^2$ .  $k_1$  is the rate constant for the pseudo-first-order kinetic model (1/min).  $k_2$  is the rate constant for the pseudo-second-order kinetic model (g mg<sup>-1</sup> min<sup>-1</sup>).  $k_i$

is the rate constant for the intraparticle diffusion (mg g<sup>-1</sup> min<sup>-1/2</sup>).  $\alpha$  is the initial adsorption rate (mg g<sup>-1</sup> min<sup>-1</sup>).  $\beta$  is a constant related with the extent of surface coverage and activation energy for chemisorptions (g mg<sup>-1</sup>). All of the graphics obtained using these kinetic models are shown in Fig. 11.

All of the isotherm parameters were calculated from the linear regression analyses of all plots in Fig. 11, and they are given in Table 4.

The values of  $q_e$  and  $k_1$  were determined from the slope and the intercept of the plots of  $\log(q_e - q_t)$  vs.  $t$  in Fig. 11(a), respectively. If it is noticed to Table 4, it was seen that the values of the  $r^2$  obtained for the pseudo-first-order kinetics were between 0.236 and 0.357 for the initial dye concentrations between 20 and 100 mg L<sup>-1</sup>. The very low values of the  $r^2$  indicate that there is not any congruity to the pseudo-first-order kinetic model.

The values of  $q_e$  and  $k_2$  were calculated the slope and the intercept of the linear plots of  $t/q_t$  vs.  $t$  in Fig. 11(b), respectively. The values of  $k_2$  were determined to be 1.585, 0.448, 0.516, 0.455, and 0.144 g mg<sup>-1</sup> min<sup>-1</sup> for the initial concentrations of 20, 40, 60, 80, and 100 mg L<sup>-1</sup>, respectively. The values of the  $r^2$  obtained for the pseudo-second-order kinetics model were found to be 1 for all concentrations. On the other hand, it was seen that the values of theoretical  $q_e$  estimated from the pseudo-second-order kinetic model was in consistent with the experimental data,  $q_e$  (exp). Because of the high values of the  $r^2$  and of a congruity between the theoretical  $q_e$  and experimental  $q_e$  (exp), it can be said that adsorption obeys the pseudo-second-order kinetic model. A similar result has also been reported for the biosorption of the BG4 onto pineapple leaf powder (*Ananas comosus*) [18].

The values of  $k_i$  and  $C$  were determined from the slope and the intercept of the plots of  $q_t$  against  $t^{1/2}$  in

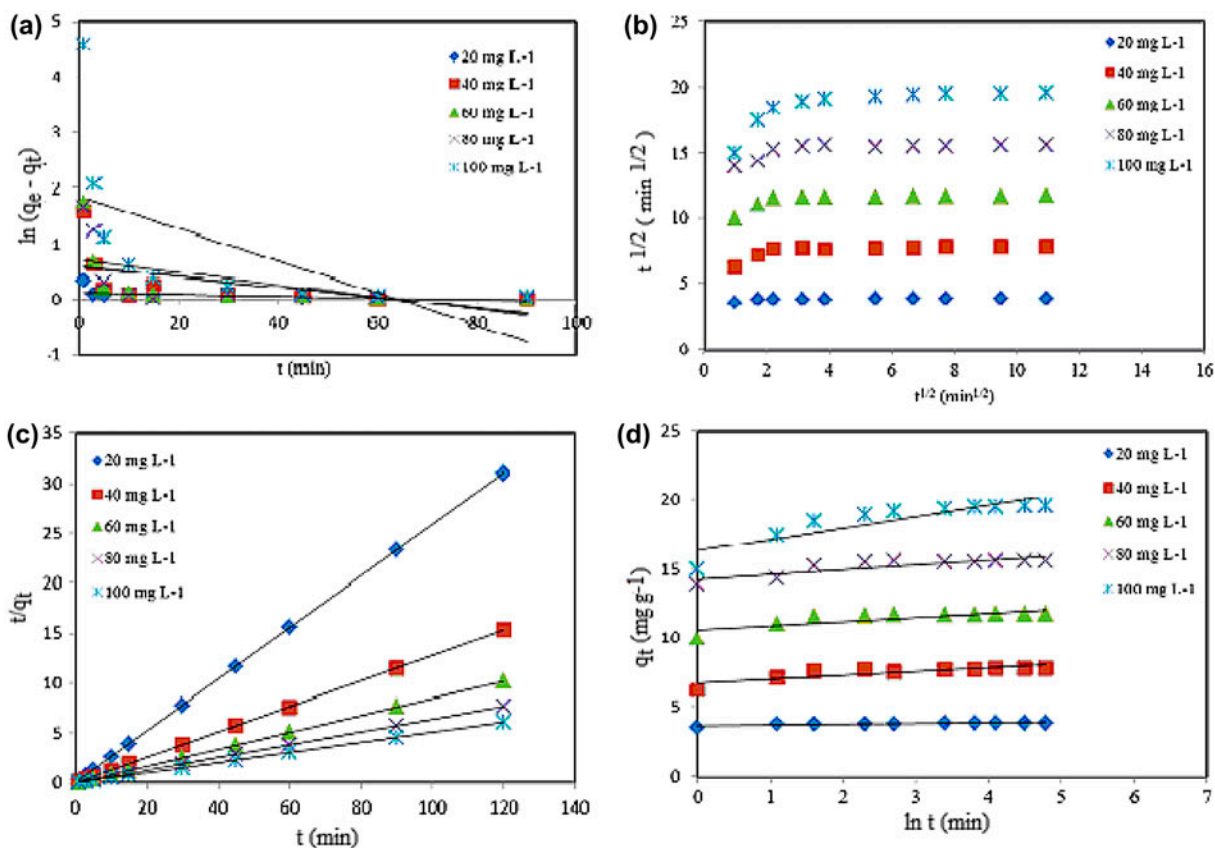


Fig. 11. The kinetic plots of the adsorption at different concentrations: (a) the pseudo first-order plots, (b) the pseudo-second-order plots, (c) the intra-particle diffusion plots, and (d) Elovic kinetic plots.

Fig. 11(c), respectively. As seen in Table 4, the values of the  $k_i$  were found to be between 0.017 and 0.30  $\text{mg g}^{-1} \text{min}^{-2}$  for the initial dye concentrations between 20 and 100  $\text{mg L}^{-1}$ , and the values of the  $r^2$  were between 0.393 and 0.503. From the results obtained, it was seen that the adsorption process did not obey the intraparticle diffusion kinetics.

The values of  $\beta$  and  $\alpha$  were determined from the slope and the intercept of the plots of  $q_t$  vs.  $\ln t$  in Fig. 11(d), respectively. The values of  $\alpha$ ,  $\beta$ , and  $r^2$  obtained are given in Table 4. The values of the  $r^2$  from the Elovic kinetic model were found to be between 0.477 and 0.787 for the initial concentrations between 20 and 100  $\text{mg L}^{-1}$ . The low values of the  $r^2$  indicate that the adsorption do not obey the Elovic kinetic model. This situation suggests that a chemical adsorption does not occur on a heterogeneous adsorbent surface [57].

### 3.12. Thermodynamic studies

In order to better understand the effect of temperature on an adsorption process, it is important to study

the thermodynamic parameters of the adsorption. Herein, the thermodynamics of the adsorption were studied using the equilibrium data obtained at temperatures of 20, 30, 40, and 50°C for the initial dye concentrations of 80  $\text{mg L}^{-1}$  at pH 4.5 and 400 rpm, respectively. Thermodynamic parameters with regard to the adsorption of the BG4 onto the OP are calculated from the following equations [63,64].

$$\Delta G^\circ = -RT \ln K_c \quad (9)$$

$$K_c = C_{Ae}/C_{Se} \quad (10)$$

$$\ln K_c = \frac{-\Delta H^\circ_{\text{ads}}}{RT} + \frac{\Delta S^\circ}{R} \quad (11)$$

where  $K_c$  is the equilibrium constant.  $C_{Ae}$  and  $C_{Se}$  are the concentrations of the dye on the adsorbent and in solution ( $\text{mg L}^{-1}$ ) at the equilibrium time, respectively.  $\Delta G^\circ$  is standard Gibbs free energy change,  $\Delta H^\circ$  is standard enthalpy change, and  $\Delta S^\circ$  is standard entropy change.  $R$  is the ideal gas constant.

Table 4  
Kinetic parameters for the adsorption of the BG4 onto the OP

$C_o$ (mg L <sup>-1</sup> )	Pseudo-first-order kinetics			Pseudo-second-order kinetics			Intraparticle diffusion		Elovic kinetics				
	$q_e$ (mg g <sup>-1</sup> )	$k_1$ (min <sup>-1</sup> )	$r^2$	$q_e$ (mg g <sup>-1</sup> )	$h$ (mg g <sup>-1</sup> min <sup>-1</sup> )	$k_2$ (g mg <sup>-1</sup> min <sup>-1</sup> )	$r^2$	$k_i$ (mg g <sup>-1</sup> min <sup>-1/2</sup> )	$C$	$\alpha$	$\beta$	$q_e^a$ (mg g <sup>-1</sup> )	
20	1.13 ± 0.04	0.001 ± 0.006	0.236 ± 0.0004	23.83 ± 0.0004	1.16 ± 0.0004	1.595 ± 0.075	1	0.018 ± 0.001	3.712 ± 0.001	0.393 ± 0.001	$6.64 \times 10^{33}$ ± 1.12	20.38 ± 0.005	0.477 ± 0.005
40	1.79 ± 0.08	0.009 ± 0.010	0.300 ± 0.0025	27.70 ± 0.0025	2.70 ± 0.0025	0.450 ± 0.040	1	0.095 ± 0.002	7.053 ± 0.023	0.429 ± 0.023	$4.25 \times 10^{10}$ ± 0.04	3.85 ± 0.002	0.698 ± 0.002
60	1.85 ± 0.02	0.009 ± 0.001	0.264 ± 0.010	73.68 ± 0.010	5.68 ± 0.010	0.535 ± 0.045	1	0.102 ± 0.002	10.89 ± 0.037	0.394 ± 0.037	$1.58 \times 10^{15}$ ± 0.06	3.48 ± 0.01	0.664 ± 0.01
80	2.04 ± 0.49	0.110 ± 0.001	0.310 ± 0.025	143.4 ± 0.025	73.90 ± 0.025	0.585 ± 0.30	1	0.117 ± 0.037	14.59 ± 0.222	0.451 ± 0.222	$3.36 \times 10^{25}$ ± 0.81	3.34 ± 0.005	0.711 ± 0.005
100	6.41 ± 0.74	0.028 ± 0.001	0.357 ± 0.055	60.55 ± 0.055	18.11 ± 0.055	0.155 ± 0.045	1	0.299 ± 0.038	17.06 ± 0.180	0.503 ± 0.180	$1.03 \times 10^{10}$ ± 0.18	1.26 ± 0.05	0.787 ± 0.05

<sup>a</sup>Experimental adsorption capacity.

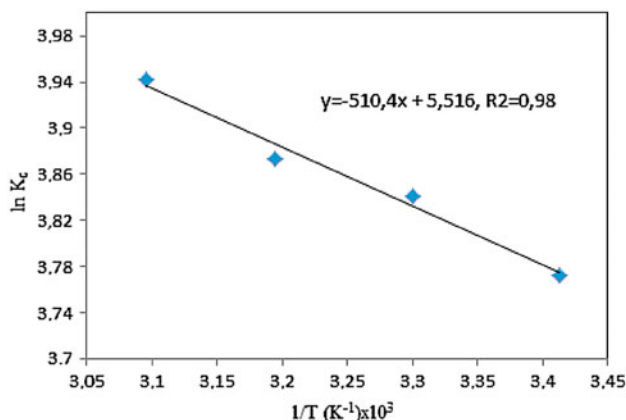


Fig. 12. Van't Hoff graph of the adsorption.

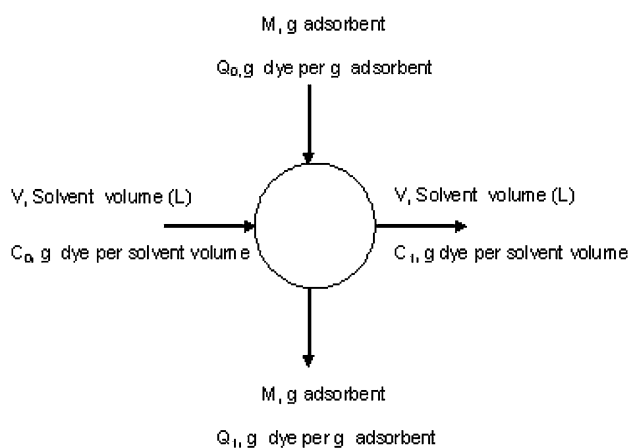


Fig. 13. Single-stage batch adsorber design.

The values of  $K_c$  and  $\Delta G^\circ$  are calculated from Eqs. (9) and (10). The Eq. (11) is known as Van't Hoff equation, the plot of  $\ln K_c$  vs.  $1/T$  according to Van' Hoff equation is shown in Fig. 12. The values of  $\Delta H^\circ$  and  $\Delta S^\circ$  are determined from the slope and intercept of this plot, respectively. The thermodynamic parameters estimated from the Van't Hoff plot for the adsorption of the BG4 onto the OP are given in Table 5.

As seen in Table 5, the negative values of  $\Delta G^\circ$  indicates the spontaneous nature of the adsorption process. The values of  $\Delta H^\circ$  and  $\Delta S^\circ$  were calculated as  $4.24 \text{ kJ mol}^{-1}$  and  $45.8 \text{ J mol}^{-1} \text{ K}^{-1}$ , respectively. The positive value of  $\Delta H^\circ$  indicates to the endothermic nature of the adsorption. Namely, the adsorption is in favor of increasing temperature. The positive value of  $\Delta S^\circ$  indicates to an increasing randomness adsorption between the OP and BG4 molecules. Similar values of

negative  $\Delta G^\circ$ , the positive  $\Delta H^\circ$  and  $\Delta S^\circ$  have also been reported for the adsorption of Malachite green on bentonite [57], for the removal of Remazol Brilliant Blue R by both the polyurethane foam [65] and the pirina [46].

### 3.13. Single-stage batch adsorber design

The design of the single-stage batch adsorption process for the adsorption of the BG4 onto the OP is illustrated in Fig. 13.

If  $g$  adsorbent ( $M$ ) is added to a certain volume of dye solution ( $L$ ), the initial dye concentration ( $C_o$ ) is reduced to  $C_1$ . Moreover, the amount of dye adsorbed per  $g$  adsorbent ( $Q_o$ ) is increased to ( $Q_1$ ) [66]. Therefore, a mass-balance equation sets up between the concentration of dye removed from the liquid and the amount of adsorbate adsorbed by the adsorbent. The mass balance equation for the system in Fig. 13 can be written as follows:

$$V(C_o - C_1) = M(Q_1 - Q_o) = M Q_1 \quad (12)$$

where  $V$  is the volume of dye solution.  $C_o$  is the initial concentration of dye solution.  $C_1$  is

concentration at any time. In the case of the equilibrium, it can be accepted as  $C_o = C_e$  and  $Q_1 = Q_e$ , and Eq. (12) can be written as follows (Eq. 13):

$$V(C_o - C_e) = M(Q_e - Q_o) = M Q_e \quad (13)$$

If Eq. (13) is rearranged, Eq. (14) is formed as

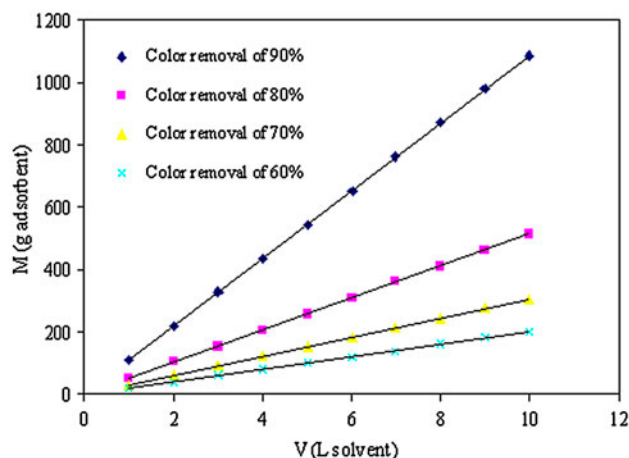
Fig. 14. Relationship between adsorbent mass ( $M$ ) and the volume of solution ( $L$ ).

Table 5

Thermodynamic parameters for the adsorption of the BG4 onto the OP

Temperature (°C)	$K_c$	$\Delta G^\circ$ (J mol <sup>-1</sup> )	$\Delta H^\circ$ (J mol <sup>-1</sup> )	$\Delta S^\circ$ (J mol <sup>-1</sup> K <sup>-1</sup> )
20	43.49	-9,190	4,243	45.80
30	46.59	-9,670		
40	48.09	-10,070		
50	51.52	-10,580		

$$M/V = C_o - C_e/Q_e \quad (14)$$

where If the coequal of  $Q_e$  from the Langmuir equation is written, Eq. (15) can be obtained as follows:

$$M/V = C_o - C_e/(Q_o b C_e / 1 + b C_e) \quad (15)$$

where  $L$  is the volume of dye solution removed by  $M$  g adsorbent. According to Eq. (15), the graph of  $M$  against  $L$  is shown in Fig. 14.

As can be seen from Fig. 14 that more mass of adsorbent will remove more dye from aqueous solution. For example, the mass of the OP required for 60, 70, 80, and 90% removal of the BG4 in a dye solution of 10 L were found as 200, 305.51, 514.12, and 1,087.50 g, respectively. If the OP is thought to be a waste agricultural material for the adsorption of dye, these results obtained is meaningful.

#### 4. Conclusions

OP and CAC were used as adsorbents for the removal of basic green four from aqueous solution by adsorption technique. The effects of contact time, initial dye concentration, temperature, pH, and ionic strength on adsorption were investigated. The adsorption increased with increasing concentration, temperature, and pH, while it was decreasing with increasing ionic strength. The experimental adsorption capacities of the CAC and the OP for the adsorption of BG4 was determined as 200 mg g<sup>-1</sup> (100%) and 19.55 mg g<sup>-1</sup> (97.75%), respectively. The Langmuir adsorption capacity ( $Q_o$ ) of the OP was found to be 41.66 mg .g<sup>-1</sup>. The adsorption was in consistent with the Langmuir, Freundlich, Temkin, and Dubinin–Raduskhevich (D–R) isotherm models and with the pseudo-second-order kinetic model. The adsorption was of spontaneous and endothermic nature. The desorption of the BG4 from the surface of the OP was very low. The adsorption had also a physical process as well as some chemical activation on the surface of the OP. The OP could be preferably used for the process

design, and it could be used as a potential adsorbent for the removal of various dyes from wastewaters.

#### Acknowledgement

This study was financially supported by The Scientific Research Projects Council of Kilis 7 Aralik University, project number: 2012/1/LTP01.

#### References

- [1] B. Acemioğlu, A. Samil, M.H. Alma, R. Gundogan, Copper(II) removal from aqueous solution by organosolv lignin and its recovery, *J. Appl. Polym. Sci.* 89 (2003) 1537–1541.
- [2] B. Acemioğlu, Adsorption of Congo red from aqueous solution onto calcium-rich fly ash, *J. Colloid Interface Sci.* 274 (2004) 371–379.
- [3] B. Acemioğlu, Removal of Fe(II) ions from aqueous solution by Calabrian pine bark wastes, *Bioresour. Technol.* 93(1) (2004) 99–102.
- [4] B. Acemioğlu, M.H. Alma, Removal of Cu(II) from aqueous solution by Calabrian pine bark wastes, *Fresenius Environ. Bull.* 13(7) (2004) 585–590.
- [5] B. Acemioğlu, M.H. Alma, A.R. Demirkiran, Removal of Zn(II) and Pb(II) ions by Calabrian pine bark wastes, *J. Chem. Soc. Pak.* 26(1) (2004) 82–89.
- [6] B. Acemioğlu, M.H. Alma, Sorption of copper(II) ions by pine sawdust, *Holz als Roh- und Werkstoff* 62 (2004) 268–272.
- [7] G. Gündoğan, B. Acemioğlu, M.H. Alma, Copper(II) adsorption from aqueous solution by herbaceous peat, *J. Colloid Interface Sci.* 269(2) (2004) 303–309.
- [8] İ. Özbay, U. Özdemir, B. Özbay, S. Veli, Kinetic, thermodynamic, and equilibrium studies for adsorption of azo reactive dye onto a novel waste adsorbent: charcoal ash, *Desalin. Water Treat.* 51 (2013) 6091–6100.
- [9] B.H. Hameed, D.K. Mahmoud, A.L. Ahmad, Sorption equilibrium and kinetics of basic dye from aqueous solution using banana stalk waste, *J. Hazard. Mater.* 158 (2008) 499–506.
- [10] M.T. Sulak, H.C. Yatmaz, Removal of textile dyes from aqueous solutions with eco-friendly biosorbent, *Desalin. Water Treat.* 37(1–3) (2012) 169–177.
- [11] B.H. Hameed, M.I. El-Khaiary, Kinetics and equilibrium studies of malachite green adsorption on rice straw-derived char, *J. Hazard. Mater.* 153 (2008) 701–708.

- [12] M. Uğurlu, Adsorption of a textile dye onto activated sepiolite, Microporous Mesoporous Mater. 119 (2009) 276–283.
- [13] B. Acemioğlu, M. Kertmen, M. Digrak, M.H. Alma, Use of *aspergillus wentii* for biosorption of methylene blue from aqueous solution, Afr. J. Biotechnol. 9(6) (2010) 874–881.
- [14] S. Chowdhury, P. Saha, Sea shell powder as a new adsorbent to remove basic green 4 (Malachite Green) from aqueous solutions: Equilibrium, kinetic and thermodynamic studies, Chem. Eng. J. 164 (2010) 168–177.
- [15] N. Sakalar, M.H. Bilir, B. Acemioğlu, M.H. Alma, Adsorption of basic red 2 onto peanut shell: Batch and column studies, Asian J. Chem. 22(5) (2010) 5649–5662.
- [16] A. Samil, B. Acemioğlu, G. Gültekin, M.H. Alma, Removal of remazol orange RGB from aqueous solution by peanut shell, Asian J. Chem. 23(7) (2011) 3224–3230.
- [17] T.K. Sen, S. Afroze, H.M. Ang, Equilibrium, kinetics and mechanism of removal of Methylene Blue from aqueous solution by adsorption onto pine cone biomass of *Pinus radiata*, Water Air Soil Pollut. 218(1–4) (2011) 499–515.
- [18] S. Chowdhury, S. Chakraborty, P. Saha, Biosorption of basic green 4 from aqueous solution by Ananas comosus (pineapple) leaf powder, Colloids Surf., B 84 (2011) 520–527.
- [19] G.M. Ratnamala, K.V. Shetty, G. Srinikethan, Removal of Remazol brilliant blue dye from dye-contaminated water by adsorption using red mud: Equilibrium, kinetic, and thermodynamic studies, Water Air Soil Pollut. 223(9) (2012) 6187–6199.
- [20] H. Karaer, I. Uzun, Adsorption of basic dyestuffs from aqueous solution by modified, Desalin. Water Treat. 51 (2013) 2219–2305.
- [21] C.T. Weber, E.L. Foletto, L. Meili, Removal of tannery dye from aqueous solution using papaya seed as an efficient natural biosorbent, Water Air Soil Pollut. 224 (2013) 1427.
- [22] E.A. Moawed, Effect of heating processes on *Salvadora persica* (Miswak) and its application for removal and determination of aniline blue from wastewater, J. Taibah Univ. Sci. 7 (2013) 26–34.
- [23] M.K. Dahri, M.R.R. Kooh, L.B.L. Lim, Water remediation using low cost adsorbent walnut shell for removal of malachite green: Equilibrium, kinetics, thermodynamic and regeneration studies, J. Environ. Chem. Eng. 2 (2014) 1434–1444.
- [24] H. Daraei, A. Mittal, M. Noorisepehr, J. Mittal, Separation of chromium from water samples using eggshell powder as a low-cost sorbent: kinetic and thermodynamic studies, Desalin. Water Treat. 53 (2015) 214–220.
- [25] H. Daraei, A. Mittal, J. Mittal, H. Kamali, Optimization of Cr(VI) removal onto biosorbent eggshell membrane: experimental & theoretical approaches, Desalin. Water Treat. 52 (2014) 1307–1315.
- [26] Mu. Naushad, A. Mittal, M. Rathore, V. Gupta, Ion-exchange kinetic studies for Cd(II), Co(II), Cu(II), and Pb(II) metal ions over a composite cation exchanger, Desalin. Water Treat. 54 (2015) 2883–2890.
- [27] J. Mittal, D. Jhare, H. Vardhan, A. Mittal, Utilization of bottom ash as a low-cost sorbent for the removal and recovery of a toxic halogen containing dye eosin yellow, Desalin. Water Treat. 52 (2014) 4508–4519.
- [28] R.N. Goyal, A. Kumar, A. Mittal, Oxidation chemistry of adenine and hydroxyadenines at pyrolytic graphite electrodes, J. Chem. Soc., Perkin Trans. 2 (1991) 1369–1375.
- [29] A. Mittal, L. Kurup, Column operations for the removal and recovery of a hazardous dye acid red 27 from aqueous solutions, using waste materials—Bottom ash and de-oiled soya, Ecol. Environ. Conversation Paper 12(2) (2006) 181–186.
- [30] J. Mittal, V. Thakur, A. Mittal, Batch removal of hazardous azo dye Bismark Brown R using waste material hen feather, Ecol. Eng. 60 (2013) 249–253.
- [31] J. Mittal, A. Mittal, Green Chemistry for Dyes Removal from Wastewater: Research Trends and Applications, Chapter 11: Hen Feather, A Remarkably Adsorbent for Dye Removal, First ed., Wiley, Scrivener Publishing LLC, USA, 2015.
- [32] G. Sharma, M. Naushad, D. Pathania, A. Mittal, G.E. El-desoky, Modification of Hibiscus cannabinus fiber by graft copolymerization: Application for dye removal, Desalin. Water Treat. 54(11) (2015) 3114–3121.
- [33] D. Bouknana, B. Hammouti, M. Messali, A. Aouniti, M. Sbaa, Olive pomace extract (OPE) as corrosion inhibitor for steel in HCl medium. Asian Pac. J. Trop. Dis. 4(S2) (2014) S963–S974.
- [34] M. Uğurlu, A. Gürses, Ç. Doğar, Adsorption studies on the treatment of textile dyeing effluent by activated carbon prepared from olive stone by ZnCl<sub>2</sub> activation, Color. Technol. 123 (2007) 106–114.
- [35] Ö. Görel, E. Kırmacı, İ. Doymaz, N.A. Akgün, Evaluation of olive oil factory wastes, Chem. Technol. 26 (2003) 40–47 (in Turkish).
- [36] F. Pagnanelli, S. Mainelli, F. Vegliò, L. Toro, Heavy metal removal by olive pomace: Biosorbent characterisation and equilibrium modelling, Chem. Eng. Sci. 58 (2003) 4709–4717.
- [37] I. Kula, M. Uğurlu, H. Karaoğlu, A. Çelik, Adsorption of Cd(II) ions from aqueous solutions using activated carbon prepared from olive stone by ZnCl<sub>2</sub> activation, Bioresour. Technol. 99 (2008) 492–501.
- [38] A. Aziz, M.S. Ouali, H. Elandaloussi, L.C. De Menorval, M. Lindheimer, Chemically modified olive stone: A low-cost sorbent for heavy metals and basic dyes removal from aqueous solutions, J. Hazard. Mater. 163(1) (2009) 441–447.
- [39] K. Rouibah, A.H. Meniai, M.T. Rouibah, L. Deffous, M.B. Lehocine, Elimination of chromium(VI) and cadmium(II) from aqueous solutions by adsorption onto olive stones, Open Chem. Eng. J. 3 (2009) 41–48.
- [40] L.M. Nieto, S.B. Alami, G. Hodaifa, C. Faur, S. Rodríguez, J.A. Giménez, J. Ochando, Adsorption of iron on crude olive stones, Ind. Crops Prod. 32 (2010) 467–471.
- [41] G. Hodaifa, J.M. Ochando-Pulido, S.B. Driss Alami, S. Rodriguez-Vives, A. Martinez-Ferez, Kinetic and thermodynamic parameters of iron adsorption onto olive stones, Ind. Crops Prod. 49 (2013) 526–534.
- [42] M. Uğurlu, A. Gürses, M. Açıkyıldız, Comparison of textile dyeing effluent on adsorption commercial activated carbon and activated carbon prepared olive



- stone by  $ZnCl_2$  activation, Microporous Mesoporous Mater. 111 (2008) 228–235.
- [43] T. Akar, I. Tosun, Z. Kaynak, E. Ozkara, O. Yeni, E.N. Sahin, S. Tunalı Akar, An attractive agro-industrial by-product in environmental cleanup: Dye biosorption potential of untreated olive pomace, *J. Hazard. Mater.* 166 (2009) 1217–1225.
- [44] R. Baccar, P. Blázquez, J. Bouzid, M. Feki, M. Sarrà, Equilibrium, thermodynamic and kinetic studies on adsorption of commercial dye by activated carbon derived from olive-waste cakes, *Chem. Eng. J.* 165 (2010) 457–464.
- [45] M. Öncel, İ. Güvenç, B. Acemioğlu, Use of pirina pretreated with hydrochloric acid for the adsorption of methyl violet from aqueous solution, *Asian J. Chem.* 24(4) (2012) 1698–1704.
- [46] S. Dağdelen, B. Acemioğlu, E. Baran, O. Koçer, Removal of Remazol brilliant blue R from aqueous solution by pirina pretreated with nitric acid and commercial activated carbon, *Water Air Soil Pollut.* 225(3) (2014) 1899.
- [47] Anonim, TAPPI Test Methods, Tappi Press, Atlanta, GA, USA, 1998.
- [48] A. Ergene, K. Ada, S. Tan, H. Katiırcioğlu, Removal of Remazol brilliant blue R dye from aqueous solutions by adsorption onto immobilized *Scenedesmus quadricauda*: Equilibrium and kinetic modeling studies, *Desalination* 249 (2009) 1308–1314.
- [49] G. Bayramoğlu, M.Y. Yakup Arıca, Biosorption of benzidine based textile dyes “Direct blue 1 and Direct red 128” using native and heat-treated biomass of *Trametes versicolor*, *J. Hazard. Mater.* 143 (2007) 135–143.
- [50] S.D. Khattri, M.K. Singh, Removal of malachite green from dye wastewater using neem sawdust by adsorption, *J. Hazard. Mater.* 167 (2009) 1089–1094.
- [51] A. Witek-Krowiak, Analysis of influence of process conditions on kinetics of malachite green biosorption onto beech sawdust, *Chem. Eng. J.* 171 (2011) 976–985.
- [52] B.H. Hameed, M.I. El-Khaiary, Malachite green adsorption by rattan sawdust: Isotherm, kinetic and mechanism modeling, *J. Hazard. Mater.* 159 (2008) 574–579.
- [53] M.S. Nityanand, M.K. Atul, C. Peter, R. Elmar, Biosorption of dyes using dead macro fungi: Effect of dye structure, ionic strength and pH, *Bioresour. Technol.* 97(3) (2006) 512–521.
- [54] Y.C. Wong, Y.S. Szeto, W.H. Cheung, G. McKay, Adsorption of acid dyes on chitosan-equilibrium isotherm analyses, *Process Biochem.* 39 (2004) 693–702.
- [55] S.N. Milmile, J.V. Pande, S. Karmakar, A. Bansawal, T. Chakrabarti, R.B. Biniwale, Equilibrium isotherm and kinetic modeling of the adsorption of nitrates by anion exchange Indion NSSR resin, *Desalination* 276 (2011) 38–44.
- [56] A. Mittal, D. Jhare, J. Mittal, Adsorption of hazardous dye Eosin yellow from aqueous solution onto waste material De-oiled soya: Isotherm, kinetics and bulk removal, *J. Mol. Liq.* 179 (2013) 133–140.
- [57] E. Bulut, M. Özacar, İ.A. Şengil, Adsorption of malachite green onto bentonite: Equilibrium and kinetic studies and process design, *Microporous Mesoporous Mater.* 115 (2008) 234–246.
- [58] S. Lagergren, About the theory of so-called adsorption of soluble substance, *Kung SvenVeten Hand* 24 (1898) 1–39.
- [59] Y.S. Ho, G. McKay, Sorption of dye from aqueous solution by peat, *Chem. Eng. J.* 70 (1998) 115–124.
- [60] Y.S. Ho, G. McKay, Pseudo-second order model for sorption processes, *Process Biochem.* 34 (1999) 451–465.
- [61] W.J. Weber, J.C. Morris, Kinetics of adsorption on carbon from solution, *J. Saint. Eng. Div. ASCE* 89(SA2) (1963) 31–39.
- [62] O. Hamdaoui, F. Saoudi, M. Chiha, E. Naffrechoux, Sorption of malachite green by a novel sorbent, dead leaves of plane tree: Equilibrium and kinetic modeling, *Chem. Eng. J.* 143 (2008) 73–84.
- [63] B. Acemioğlu, M.H. Alma, Equilibrium studies on adsorption of Cu(II) from aqueous solution onto cellulose, *J. Colloid Interface Sci.* 243 (2001) 81–84.
- [64] M. Hema, S. Arivoli, Comparative study on the adsorption kinetics and thermodynamics of dyes onto acid activated low cost carbon, *Int. J. Phys. Sci.* 2(1) (2007) 10–17.
- [65] M.H. Bilir, N. Şakalar, B. Acemioğlu, E. Baran, M.H. Alma, Sorption of Remazol brilliant blue R onto polyurethane-type foam prepared from peanut shell, *J. Appl. Polym. Sci.* 127 (2013) 4340–4351.
- [66] V. Vadivelan, K. Kumar, Equilibrium, kinetics, mechanism, and process design for the sorption of methylene blue onto rice husk, *J. Colloid Interface Sci.* 286 (2005) 90–100.
- [67] R. Han, Y. Wang, Q. Sun, L. Wang, J. Song, X. He, C. Dou, Malachite green adsorption onto natural zeolite and reuse by microwave irradiation, *J. Hazard. Mater.* 175 (2010) 1056–1061.
- [68] Y.C. Sharma, B. Singh, Uma, Fast removal of Malachite Green by adsorption on rice husk activated carbon, *Open Environ. Pollut. Toxicol. J.* 1 (2009) 74–78.
- [69] S.S. Tahir, N. Rauf, Removal of a cationic dye from aqueous solutions by adsorption onto bentonite clay, *Chemosphere* 63 (2006) 1842–1848.